Applied Catalysis B: Environmental 88 (2009) 564–575

Contents lists available at ScienceDirect

Applied Catalysis B: Environmental

journal homepage: www.elsevier.com/locate/apcatb

Effect of ethyleneglycol addition on the properties of P-doped NiMo/Al_2O_3 HDS catalysts: Part I. Materials preparation and characterization

José Escobar [a,*], María C. Barrera [a], José A. Toledo [a], María A. Cortés-Jácome [a], Carlos Angeles-Chávez [a], Sara Núñez [b], Víctor Santes [c], Elizabeth Gómez [d], Leonardo Díaz [a], Eduardo Romero [a], José G. Pacheco [e]

[a] Instituto Mexicano del Petróleo, Eje Central Lázaro Cárdenas 152, San Bartolo Atepehuacan, Gustavo A. Madero, México, D.F. 07730, Mexico
[b] Departamento de Ingeniería de Procesos e Hidráulica, Universidad Autónoma Metropolitana-Iztapalapa, San Rafael Atlixco 186, México, D. F. 09340, Mexico
[c] Depto. de Biociencias e Ingeniería, CIIEMAD-IPN, Calle 30 de Junio de 1520, Col. Barrio la Laguna Ticomán, Gustavo A. Madero, México, D.F. 07340, Mexico
[d] Instituto de Química, Universidad Nacional Autónoma de México, Circuito Exterior, Ciudad Universitaria, México, D.F. 04510, Mexico
[e] División Académica de Ciencias Básicas, Universidad Juárez Autónoma de Tabasco, Km. 1, Carretera Cunduacán-Jalpa de Méndez, Cunduacán, Tabasco, Mexico

ARTICLE INFO

Article history:
Received 6 July 2008
Received in revised form 8 October 2008
Accepted 9 October 2008
Available online 21 October 2008

Keywords:
Ethyleneglycol
Phosphomolybdates
Hydrodesulfurization
NiMo/Al_2O_3 catalyst
NiMoS phase
ULSD

ABSTRACT

Phosphorous-doped NiMo/Al_2O_3 hydrodesulfurization (HDS) catalysts (nominal Mo, Ni and P loadings of 12, 3, and 1.6 wt%, respectively) were prepared using ethyleneglycol (EG) as additive. The organic agent was diluted in aqueous impregnating solutions obtained by MoO_3 digestion in presence of H_3PO_4, followed by $2NiCO_3{\cdot}3Ni(OH)_2{\cdot}4H_2O$ addition. EG/Ni molar ratio was varied (1, 2.5 and 7) to determine the influence of this parameter on the surface and structural properties of synthesized materials. As determined by temperature-programmed reduction, ethyleneglycol addition during impregnation resulted in decreased interaction between deposited phases (Mo and Ni) and the alumina carrier. Dispersion and sulfidability (as observed by X-ray photoelectron microscopy) of molybdenum and nickel showed opposite trends when incremental amounts of the organic were added during catalysts preparation. Meanwhile Mo sulfidation was progressively decreased by augmenting EG concentration in the impregnating solution, more dispersed sulfidic nickel was evidenced in materials synthesized at higher EG/Ni ratios. Also, enhanced formation of the so-called "NiMoS phase" was registered by increasing the amount of added ethyleneglycol during simultaneous Ni–Mo–P–EG deposition over the alumina carrier. That fact was reflected in enhanced activity in liquid-phase dibenzothiophene HDS (batch reactor, $T = 320\ ^\circ C$, $P = 70\ kg/cm^2$) and straight-run gas oil desulfurization (steady-state flow reactor), the latter test carried out at conditions similar to those used in industrial hydrotreaters for the production of ultra-low sulfur diesel ($T = 350\ ^\circ C$, $P = 70\ kg/cm^2$, LHSV = 1.5 h^{-1} and H_2/oil = 2500 ft^3/bbl).
© 2008 Elsevier B.V. All rights reserved.

1. Introduction

Fulfilment of very stringent regulations regarding S content (i.e., ~10–15 ppm for diesel) in fuels obtained from oil-derived middle distillates hydrotreatment requires improved processes and more active hydrodesulfurization (HDS) catalysts [1]. In this context, the use of various types of organic additives during catalyst preparation has resulted in materials of enhanced S removal activity. For example, different beneficial effects have been related to chelators addition due to their strong interaction with the promoter metals (Ni and Co) to deposit [2]. It has been determined [2,3] that those organic compounds delay promoter sulfidation to temperatures high enough to permit efficient integration of sulfidic Co or Ni species to then already formed MoS_2 (or WS_2), thus optimizing promoted phases ("NiMoS" or "CoMoS") formation. It could be stated that the origin of the enhanced HDS activity of catalysts prepared in presence of chelating ligands is rather well-established [4].

Regarding the effect of glycols as HDS catalysts additive the scenario is different. It could be said that, so far, there is no general agreement about the origin of their beneficial influence on the hydrodesulfurizating properties of otherwise conventional CoMo or NiMo alumina-supported materials. Although utilization of those organic additives in improving hydrotreating catalysts has been previously patented [5,6] just a few reports related to their use in improving those formulations are available in the open literature. Prins and co-workers [7] synthesized Al_2O_3-supported CoMo catalysts (doped with phosphate) in

* Corresponding author. Tel.: +52 55 9175 8389; fax: +52 55 9175 6380.
E-mail address: jeaguila@imp.mx (J. Escobar).

0926-3373/$ – see front matter © 2008 Elsevier B.V. All rights reserved.
doi:10.1016/j.apcatb.2008.10.005

presence of tri-ethyleneglycol, ethyleneglycol and tri-ethyleneglycol dimethyl ether, the resulting materials being tested in thiophene HDS. The catalysts containing either ethyleneglycol or tri-ethyleneglycol and phosphorous (simultaneously impregnated with Mo and Co) showed a ~70% increase in activity, as compared to the material with no additives. Even more, a synergistic effect of simultaneous glycols and P addition was observed, the influence of both agents on effectively promote HDS activity being higher when added together. It was proposed that the organic compound interacts with both basic OH groups and coordinatively unsaturated Al^{3+} sites on the alumina surface preventing decomposition of Co diphosphopentamolybdate complexes (present in the impregnating solution) during their deposition on the carrier. Thus, close proximity of Co and Mo in those impregnated complexes could result in enhanced formation of the so-called "CoMoS phase" during sulfiding. The aforementioned authors also registered increased molybdenum sulfidability in $CoMo/Al_2O_3$ material impregnated in presence of tri-ethyleneglycol [8]. Other authors [9] have also proposed optimized promoter integration to MoS_2 phase in HDS catalysts prepared in presence of glycols as origin of important improvements in catalytic activity (in tetraline hydrogenation and 4,6-dimethyldibenzothiophene HDS), as to that of conventional formulations with no organic additive. In this case, the di-ethyleneglycolbutylether added (at Mo/organic additive = 0.75) seemed to slow-down Mo and Co sulfidation at temperatures up to 200 °C, its influence (differently to that observed for chelating ligands) being more important on the former. Interestingly, those authors deposited the organic additive on a previously impregnated industrial alumina-supported Co–Mo–P formulation. Then, the role of glycols must have been different to that they exerted when simultaneously impregnated with Mo, Co and P [7,8]. Other group reported [10] that toluene hydrogenation was more strongly enhanced over $CoMo/Al_2O_3$ formulations (with or without phosphorous) when the additive (tri-ethyleneglycol) was impregnated on dried impregnated precursors, instead of on the corresponding calcined materials. Iwamoto et al. [11] also determined a beneficial effect of simultaneously impregnating polyethylene glycol (PEG), Mo and Co on alumina carrier. The prepared materials had higher activity (in thiophene, dibenzothiophene and light gas oil HDS) than a reference conventional sulfided catalyst of similar composition prepared with no organic agent. After characterizing the solids by various instrumental techniques the authors concluded that polyethylene glycol addition promoted better sulfided phases dispersion by hindering their sintering. In the opposite to that carried out during the other aforementioned investigations, Iwamoto et al. [11] submitted the impregnated solids (modified by PEG addition) to calcining (at 550 °C) precluding any effect of the organic additive (which was thus decomposed by combustion) during the sulfiding of either cobalt or molybdenum. Considering that reported in the pertinent literature, it could be concluded that the magnitude of the effect of glycols on HDS properties depends on the preparation step where they are added. Also, it must not be discarded that the positive influence of those organic species on the HDS activity of corresponding catalysts could be related to several independent phenomena.

To try to contribute in elucidating the effect of ethyleneglycol (EG) addition on HDS catalyst properties, in this work we prepared P-doped $NiMo/Al_2O_3$ materials using that additive at various amounts (EG/Ni molar ratios of 1, 2.5 and 7). Materials characterization included N_2 physisorption, X-ray diffraction, thermal analysis (TG and DTA), Fourier transformed infrared spectroscopy (FTIR) and temperature-programmed reduction. Sulfided catalysts were studied by high-resolution transmission electron microscopy and X-ray photoelectron spectroscopy. Catalytic activity of selected samples was tested in both model compound (dibenzotiophene) HDS and real feedstock (straight-run gas oil) desulfurization.

2. Experimental

2.1. Catalysts synthesis

High surface area alumina was obtained from calcining a commercial boehmite (Versal 200 from Euro Support) at 500 °C (5 h). The textural properties (as determined by N_2 physisorption) of the final Al_2O_3 carrier were surface area (S_g) = 307 m^2/g, pore volume (V_p) = 0.9 cm^3/g and average pore diameter (from $4 \times V_p/S_g$) ~12 nm. Texture of this support seemed to be especially suitable for its application as carrier of catalysts for the hydrotreatment of middle distillates [12]. Previously to impregnation, the support was dried at 120 °C (2 h) to eliminate physisorbed water. Pore-filling simultaneous impregnation was carried out by using an aqueous solution (pH ~ 1.4) prepared from digestion (at ~80 °C under vigorous stirring) of MoO_3 99.5 wt% (PQM) in presence of H_3PO_4 85.3 wt% (Tecsiquim). After 2 h, a yellow transparent solution was observed. $2NiCO_3{\cdot}3Ni(OH)_2{\cdot}4H_2O$ (Sigma–Aldrich) was then added, heating being maintained for 2 h. Ni concentration corresponded to Ni/(Ni + Mo) = 0.29 whereas the ratio $P_2O_5/(NiO + MoO_3)$ = 0.1 (mass ratio) was fulfilled [13]. Molar concentrations of Mo, Ni and P in impregnating solutions corresponded to 1.67, 0.68 and 0.69, respectively. A transparent emerald green solution was thus obtained. Ethyleneglycol (EG, J.T. Baker) at various EG/Ni molar ratio (EG/Ni = 1, 2.5 and 7) was added to the final impregnating solution which pH was essentially not altered after this step (final pH ~1.6). Nominal Mo, Ni and P loadings corresponded to 12, 3 and 1.6 wt% in final catalyst, respectively. After impregnation materials were dried at 120 °C (2 h). Calcining was avoided to preserve organic additive integrity. Samples were identified by using the NMP(x) key where "x" represented the EG/Ni ratio. A reference material with no organic additive, sample NMP(0), was also synthesized. This solid was dried at 120 °C (2 h), calcining being avoided. Sulfided catalysts were obtained by submitting impregnated precursors to treatment at 400 °C (heating rate 6 °C/min) under H_2/H_2S (Praxair) at 50 ml/min/6 ml/min during 2 h.

2.2. Materials characterization

Textural properties of various materials were determined by N_2 physisorption (at −196 °C), in a Micromeritics ASAP 2000 apparatus. Surface area and pore size distribution of the alumina support were determined by BET and BJH (N_2 adsorption branch data) protocols, respectively. Structural order was studied by powder X-ray diffraction (Siemens D-500 Kristalloflex, Cu Kα radiation, λ = 0.15406 nm, 35 kV, 25 mA). Thermal analyses were carried out with a Netzch Thermische Analize, STA 409 EP apparatus under static air atmosphere. Diffuse reflectance infrared Fourier transform spectroscopy (DRIFTS) of various materials was performed by using a Bruker TENSOR 27 instrument. Samples (in KBr) were placed in a cup inside a diffuse reflectance unit. Spectra were averaged over 40 scans in the 210–4000 cm^{-1} range to a nominal 4 cm^{-1} resolution. Spectra taken are presented in the Kubelka–Munk format. Temperature-programmed reduction (TPR) experiments were conducted by using an Altamira 2000 equipment. Samples of as-made (dried) $Ni–Mo–P/Al_2O_3$ impregnated precursors, either with or without glycol, were put in a quartz reactor. Circa 50 mg of materials ground at particle size that passed through U.S. Mesh 80 (180 μm) were heated from 30 to

850 °C (at 5 °C/min, heating rate) under a 30 ml/min flow of an Ar/H_2 90/10 (vol/vol) mixture. Supported sulfidic phases were characterized by electron microscopy and X-ray photoelectron spectroscopy (XPS). Transmission electron microscopy (TEM) was performed in a JEM-2200FS at accelerating voltage of 200 kV. The apparatus was equipped with a Schottky-type field emission gun and an ultra-high resolution (UHR) configuration (Cs = 0.5 mm; Cc = 1.1 mm; point-to-point resolution, 0.19 nm) and in-column energy filter omega-type. The samples to be analyzed were ground, suspended in isopropanol at room temperature and dispersed with ultrasonic agitation. Then, some drops of the suspension were deposited on a 3 mm diameter lacey carbon copper grid. GATAN™ software was used during statistical determination of slab length and stacking degree in MoS_2-supported particles. XPS spectra were obtained in a THERMO-VG SCALAB 250 spectrometer equipped with Al Kα X-ray source (1486.6 eV) and a hemispherical analyzer. Experimental peaks were decomposed into components using mixed Gaussian–Lorentzian functions and a non-linear squares fitting algorithm. Shirley background subtraction was applied. Binding energies were reproducible to within ±0.2 eV and the C 1s peak (from adventitious carbon) at 284.6 eV was used as a reference. Surface elemental composition was determined by fitting and integrating the Ni (2p), Mo (3d), S (2s), P (2p) and Al (2p) and converting these values to atomic ratios by using theoretical sensitivity factors provided by the manufacturer of the XPS apparatus [14]. Sulfided catalysts were kept under inert atmosphere by using a glove box and a special box vessel to introduce the samples into the spectrometer analysis chamber.

3. Results and discussion

3.1. Thermal analysis and X-ray diffraction

Thermogravimetric (TG) patterns of various samples studied are shown in Fig. 1. The alumina carrier used (previously stabilized by calcining at 500 °C) did not show any important weight loss (with the sole exception of physically adsorbed water evaporation) in the temperature range studied. All analyzed materials had the aforementioned signal (a $T \sim 100$ °C) attributable to physisorbed water elimination. To try to determine the influence of adsorbed organic species on TG profile of the alumina support we impregnated ethyleneglycol (EG) in aqueous solution at concentrations equivalent to those in NMP(2.5) and NMP(7) on the carrier alone (samples EG(2.5)/Al and EG(7)/Al, respectively). The corresponding thermograms are shown in Fig. 1. Both samples presented very similar profiles each other, the final weight losses

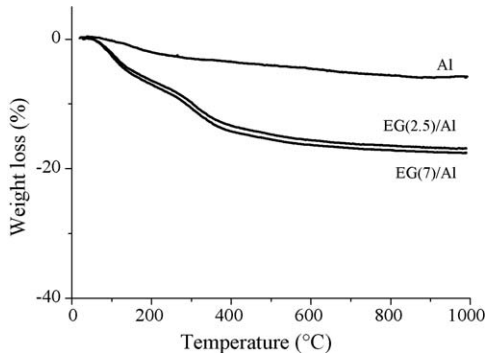

Fig. 1. Thermogravimetrical analysis (under static air atmosphere) of dried samples of Al_2O_3 carrier impregnated with ethyleneglycol at various concentrations. EG(2.5)/Al and EG(7)/Al contain ethyleneglycol at concentrations equivalent to those in NMP(2.5) and NMP(7), respectively. Thermogram of the corresponding Al_2O_3 carrier (Al) included as reference.

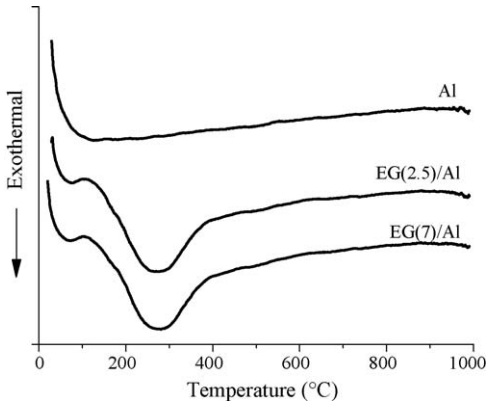

Fig. 2. Differential thermal analysis (under static air atmosphere) of dried samples of Al_2O_3 carrier impregnated with ethyleneglycol at various contents. EG(2.5)/Al and EG(7)/Al contained the organic additive at concentration corresponding to those in NMP(2.5) and NMP(7), respectively. Thermogram of Al_2O_3 carrier (Al) included as reference.

being slightly higher in the case of the material of increased EG content. Losses in the ~150–260 °C temperature range suggested elimination of both physisorbed EG (ethyleneglycol, boiling point ~197 °C) and species in weak interaction with the support. The abrupt slope change at ~261–360 °C temperature range could probably indicate the existence of more stable organic moieties. The aforementioned thermogravimetrical curves leveled off at temperature over 550 °C. It is worth mentioning that these results are very similar to those reported by Iwamoto et al. [11] in the case of alumina samples impregnated with polyethylene glycol (PEG, at 10 wt%). The corresponding differential thermal analyses (Fig. 2) showed endothermal inflections related to physisorbed species elimination. An intense exothermal signal with maximum at ~272 °C related to organic matter combustion was registered. The broadness of this inflection could be probably originated in the existence of organic species of different interaction degree with the alumina carrier. Again, our findings are alike to those presented by Iwamoto et al. [11] who identified a strong exothermicity (centered at ~247 °C) that was related to organic matter decomposition in their aforementioned samples of alumina impregnated with PEG. Saravanan and Subramanian [15] proposed that PEG (in aqueous solution) could interact with the alumina substrate (α-phase in their case) surface through three different mechanisms: (1) Brønsted acid–base interaction (hydrogen bonding) between superficial Al–OH groups and etheric oxygen of PEG, (2) coordination between Al^{3+} Lewis acidic sites and the basic oxygen of ethoxyl groups of PEG and (3) electrostatic interaction between positively charged alumina surface and feebly negatively charged ethoxy oxygen of PEG (for pH values lower than 9). As no etheric oxygen are present in EG, mechanisms (2) and (3) could mainly dictate the nature of the ethyleneglycol–alumina interaction that could take place during our adsorption experiments. Also, the very acidic conditions of the Ni–Mo–P–EG impregnation solutions used (pH ~ 1.6, see Section 2.1) could strongly favor mechanism (3). We could not discard that under the conditions used during our thermal analysis some strongly adsorbed organic species could be formed (by transformation of the original EG deposited) which combustion could originate the exothermal inflexions observed in the DTA profiles of EG/Al samples in Fig. 2.

In solids simultaneously impregnated with Ni–Mo–P–EG aqueous solution (see Fig. 3), the main signal related to organic species combustion was observed at lower temperature, as to that registered in the case of EG/Al solids (Fig. 2). The magnitude of this shift was function of ethyleneglycol content (peaks at ~240 and

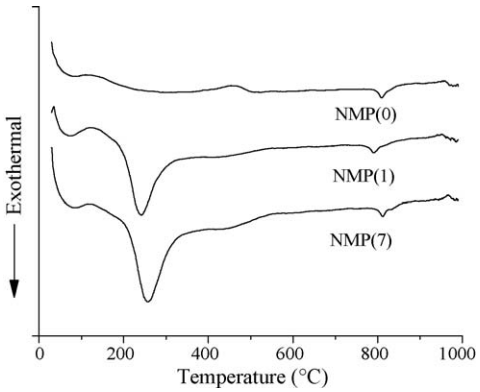

Fig. 3. Differential thermal analysis (under static air atmosphere) of dried samples of P-doped $NiMo/Al_2O_3$ samples at various EG/Ni ratios. Pattern corresponding to the dried alumina-supported Ni–Mo–P sample impregnated with no ethyleneglycol included as reference.

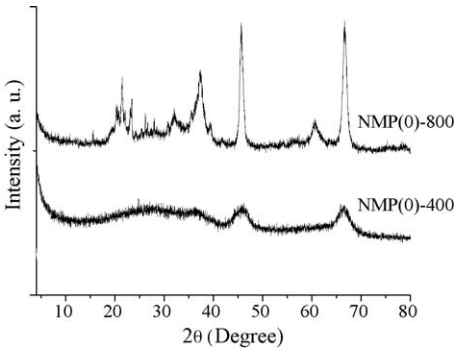

Fig. 4. X-ray diffraction patterns of P-doped $NiMo/Al_2O_3$ sample prepared with no glycol, calcined at 400 °C (4 h) and 800 °C (2 h).

~257 °C for NMP(1) and NMP(7), respectively). A similar phenomenon was registered by Iwamoto et al. [11] but no hypothesis was advanced to try to explain the observed behavior. In the past, alumina-supported Mo^{6+} materials have been tested as catalysts for organic material (diesel soot) combustion [16,17]. It has been reported [16] that in presence of samples with 11 wt% Mo soot combustion temperature (as determined by differential scanning calorimetry) could be decreased by about ~100 °C, as to that corresponding to the non-catalyzed oxidation. Regarding our impregnated samples, it could be that under the thermal analysis conditions used (under air flow) oxidic molybdenum species could catalyze organic species oxidation, this resulting in early exothermal combustion. Another exothermicity observed at higher temperature (maximum at ~438 and ~448 °C, for NMP(1) and NMP(7), respectively) suggested the existence of some refractory organic residua. Intensity of this signal increased with the ethyleneglycol concentration in the analyzed sample. It was apparent that this highly stable species were not present in EG/Al samples (Figs. 1–2) pointing out to a certain interaction between refractory organic matter and deposited phases. However, the formation of some kind of complexes between ethyleneglycol and Ni or Mo seemed to be improbable considering the weak complexing properties of that organic species [15]. In spite of that, we observed that the originally dark emerald green impregnating solution used changed its color after EG addition. After 2 days, a dark blue cobalt color was observed when Ni–Mo–P solutions (where ethyleneglycol had been added at EG/Ni = 1 and 7) were allowed to stand at room temperature. Other authors [18] have reported that Ni^{2+} complexation could be responsible for similar phenomenon (blue-shift of Ni^{2+} d–d transition bands) when H_2O molecules in the coordination sphere of hexaquonickel cations $[Ni(H_2O)_6]^{2+}$ had been displaced by ligands (ethylenediamine in this case) stronger than water in the spectrochemical series. In contrast with that we observed, other authors did not identified variations neither in color nor in pH, after adding tri-ethyleneglycol to originally reddish Co–Mo–P impregnating solutions [8]. Considering that the first step during preparation of our impregnation solutions was MoO_3 digestion (at ~80 °C) in presence of H_3PO_4 (at Mo/P ~2.5) $HP_2Mo_5O_{23}^{5-}$ (which structure consists of five interconnected octahedral MoO_6 units surrounding two PO_4 tetrahedrons [7]) species could have been formed. Whether ethyleneglycol addition could favor complexation of Ni by diphosphopentamolybdate anions [7] (by an undetermined mechanism) is a point that deserves further investigation in future communications.

There was only one defined thermal phenomenon for the formulation impregnated with Ni–Mo–P but no glycol. That high-temperature exothermal inflection (centered at ~792–810 °C) observed for all Ni–Mo–P impregnated formulations suggested supported phases crystallization. To get further insight in this phenomenon we analyzed the structural order (as determined by X-ray diffraction) of NMP(0) impregnated samples annealed at 400 °C (4 h) and 800 °C (2 h). The registered diffractograms are shown in Fig. 4. The formulation calcined at lower temperature just presented broad signals corresponding to the γ-Al_2O_3 support. The absence of defined peaks and the high noise/signal ratio evidenced highly dispersed deposited amorphous phases. After calcining under severe conditions (800 °C, 2 h), well-defined γ-Al_2O_3 and nickel aluminate ($Ni_2Al_{18}O_{29}$) phases were clearly evident. Other authors [19] have found similar results when studying alumina-supported oxidic nickel (~10 wt%) catalysts prepared in presence of organic additive (glycine) and calcined at 800 °C under static air atmosphere. In our case, $Al_2(MoO_4)_3$ crystals were also registered (main peak at $2\theta = 23.3°$) in the diffractogram corresponding to the sample annealed under severe conditions. In this line, Ma et al. [20] observed the aforementioned phase in a MoO_3/Al_2O_3 catalyst (at 14 wt% Mo) annealed at 550 °C. No peaks indicating MoO_3 presence were evidenced in our alumina-supported Ni–Mo–P sample calcined at elevated temperature. Very possibly, this fact was caused by molybdenum oxide melting and evaporation that could take place at the severe annealing conditions used [16,21]. In full accordance with this, the onset of an endothermal phenomenon (centered at ~750 and ~968 °C for NMP(1) and NMP(7), respectively) was registered in both samples at either EG content, just after the signal originated by exothermal nickel aluminate crystallization (see Fig. 3). The concomitant weight losses were clearly evident in the corresponding thermogravimetrical profiles shown in Fig. 5.

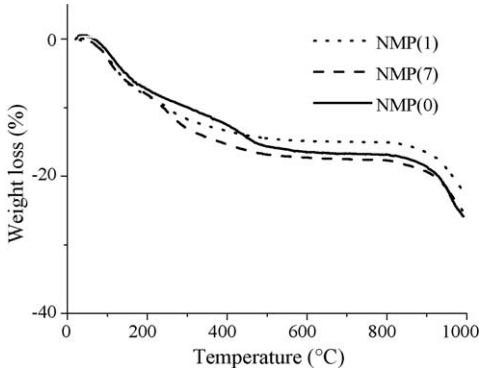

Fig. 5. Thermogravimetrical analysis (under static air atmosphere) of dried samples of P-doped $NiMo/Al_2O_3$ samples at various EG/Ni ratios. Pattern corresponding to the dried alumina-supported Ni–Mo–P sample impregnated with no ethyleneglycol included as reference.

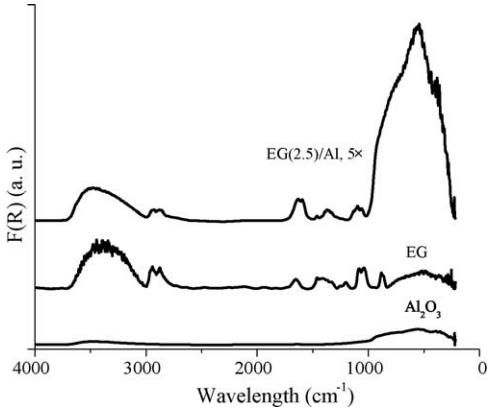

Fig. 6. FTIR spectra (Kubelka–Munk) of neat EG, the Al_2O_3 support used and of this carrier modified by EG adsorption (at EG(2.5)/Al). The last spectrum is shown at 5× magnification for sake of clarity.

3.2. Fourier-transformed infrared spectroscopy

In Fig. 6 infrared spectra corresponding to neat EG, the Al_2O_3 support used during catalyst preparation and to that carrier modified by EG adsorption (at EG(2.5)/Al) are shown. Regarding the organic compound at room temperature, a couple of bands at ~2880 and ~2945 cm^{-1}, corresponding to CH_2-symmetric stretching vibration modes are identified. In the region between 1203 and 1461 cm^{-1} bands associated with OH in-plane bending mode and the CH_2-wagging and twisting modes appeared. Bands at 1411 and 1370 cm^{-1} are almost exclusively originated by OH in-plane bending mode [22,23]. Additionally, the EG spectrum also exhibited two strong bands in the 865–880 cm^{-1} region which were assigned to C–C and C–O skeletal stretching modes, while bands at 1040 and 1082 cm^{-1} raised from the CH_2-rocking mode [22]. Regarding the spectrum of EG(2.5)/Al, the intensity of the bands related to CH_2-symmetric stretching vibration was strongly diminished (some variation in shape was also observed) as compared with those corresponding to neat ethyleneglycol (at ~2880 and ~2945 cm^{-1}). We think that this fact could be considered as compelling evidence of EG chemisorption on the support surface. Also, new bands observable at 1591 and 1632 cm^{-1} were attributable to neither the alumina support nor to neat ethyleneglycol, but to Al–O–C vibration modes [7,23,24]. The region between 1000 and 1500 cm^{-1} was also significantly changed by interaction between adsorbed EG and the Al_2O_3 carrier. It should be pointed out that in that region the bands corresponding to OH in-plane bending mode of hydroxyl groups (in EG molecule) almost vanished. This fact, in connection with the appearance of the aforementioned signals at 1591 and 1632 cm^{-1} led us to hypothesize that those OH-groups participated in formation of new Al–O–C fragments. In a recent investigation from Nicosia and Prins [7], it was reported that IR bands in the 1600–1700 cm^{-1} region corresponding to Al–O–C vibrations appeared due to EG–Al_2O_3 chemical interaction. Conversely, those authors did not observe those signals in similar samples with SiO_2 support. In that report [7], it was assumed that the most important mechanism originating the already mentioned chemical interaction took place through the basic surface OH groups of the alumina support which were sites associated to organic molecules adsorption. We assumed that IR reflectance bands observed in the 1591–1632 cm^{-1} region (due to Al–O–C vibrations) in our EG(2.5)/Al sample were originated by chemical interaction between the oxygen atom coming from hydroxyl groups of the EG molecule and Al^{3+} coordinatively unsaturated sites (CUS) on the carrier surface. In line with this, van Veen et al. [25] reported formation of Al–O–C bonds from chemical interaction between acetyl acetonate and CUS (Al^{+3}) on γ-alumina surface. In other study Ramis et al. [26] reported that various alcohols were adsorbed over titania through Lewis acid sites that were present on the TiO_2 surface. However, regarding the IR bands corresponding to OH in-plane bending mode of adsorbed complexes no significant changes were evidenced in this case [26]. Presumably, decreased intensity of these signals (as to those of non-adsorbed organic molecule) could have been evidenced formation of species coordinatively attached to the Lewis acid sites on titania. Regarding alumina surface, it has been demonstrated [27] that electronegative species (as fluoride anions, for instance) can substitute the most basic hydroxyls groups (those of higher negative charge) attached to Al^{3+} sites [28]. Following this way of reasoning, from our study it seemed that ethyleneglycol behaved as a nucleophile reacting over surface acidic sites. Although the specific type of displaced hydroxyl was not possible to distinguish, it was conceivable that EG molecules reacted over Al^{3+} surface sites. Moreover, the significant changes observed in the IR region corresponding to OH in-plane bending mode of the hydroxyls groups in EG molecules (see EG(2.5)/Al pattern in Fig. 6) supported the idea that glycol molecules were chemisorbed over Al^{3+} sites. In accordance with Nicosia and Prins [8] who found that co-impregnating with tri-ethyleneglycol resulted in weakened interaction between heptamolybdate anions and Al_2O_3 surface sites, due to the previously described mechanism strong interactions between alumina carrier sites and molybdenum-containing anions could be prevented, when contacting the support with our Ni–Mo–P–EG impregnating solutions (see Section 2.1).

Fig. 7 shows the FTIR spectra of NMP(0) and NMP(1) impregnated precursor (dried at 120 °C/2 h). The band at ~850 cm^{-1} (more visible in NMP(1) spectrum) could be originated in stretching modes of octahedral poly-molybdates [29] meanwhile in the 535–555 cm^{-1} range the one related to bending vibration of the triply degenerated O–P–O ν_4 mode corresponding to tetrahedral PO_4^{3-} units [30,31] could be observed. Remnant bands at 2880–2945 cm^{-1} assigned to ethyleneglycol (see EG spectrum in Fig. 6) were identified. This fact might be associated with that one of the hydroxyl groups of EG molecules could have reacted with Al^{3+} less-acidic coordinatively unsaturated sites being then weakly chemisorbed on the alumina surface. Also, there was the possibility that those bands could be originated by free dangling hydroxyls (from EG) remaining unreacted. Whatever the case, our results suggest that the organic additive primarily blocks Al^{3+} sites of alumina support (which react with at least one of the

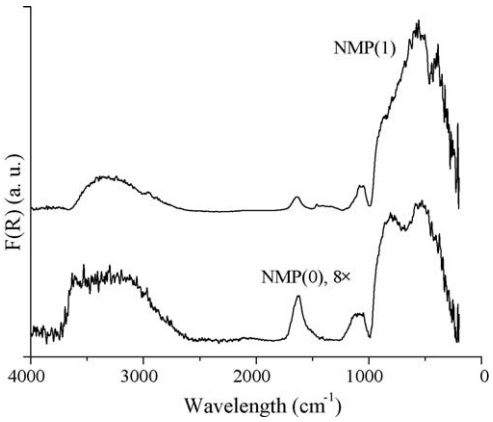

Fig. 7. FTIR spectrum (Kubelka–Munk) of dried P-doped NiMo/Al_2O_3 sample at equimolar EG/Ni ratio. Spectrum corresponding to a similar material prepared with no ethyleneglycol included as reference.

OH-groups present in the organic additive). As proposed by others [8], this could eventually lead to the formation of more sulfidable poly-molybdates species on the catalysts surface. Our FTIR spectra suggested that the existence of Al–O–P linkages (corresponding to non-stoichiometric aluminum phosphate) related to vibrations in the 846–763 cm^{-1} region [32], clearly present in NMP(0), was limited in NMP(1). As already mentioned, $HP_2Mo_5O_{23}^{5-}$ species (stable up to pH ~ 6 [33]) could be present in the impregnating solution prepared from MoO_3 digestion in presence of H_3PO_4 (see Section 2.1). During contacting with the Al_2O_3 carrier, solution pH could be increased due to characteristic properties (notably zero-charge point) of support surface. Above pH ~ 6, pentamolybdates decompose generating adsorbed phosphate and molybdate anions [34]. The former could react with acidic OH groups on the carrier surface, thus originating $AlPO_4$ (see IR band at 846–763 cm^{-1} region related to Al–O–P linkages in NMP(0) sample). On the other hand, when basic OH and Al^{3+} sites are blocked by glycol adsorption the interaction between the diphosphopentamolybdate species and the γ-Al_2O_3 carrier is affected [7]. Due to the alumina–glycol interaction, the zero-charge point of the support is modified and decomposition of those anions is diminished [7]. Then, the amount of Al–O–P bonds formed could be lowered, as to that originated in the case of similar impregnations carried out in absence of the organic additive.

3.3. Temperature-programmed reduction (TPR)

In Fig. 8 TPR profiles for various alumina-supported Ni–Mo–P impregnated precursors are shown. In all of them three main signals (corresponding to different H_2-consuming phenomena) could be clearly identified. The first peak, which progressively shifted to lower temperature as the ethyleneglycol content during impregnation was increased (see Table 1), could be associated to reduction of Mo^{6+} present in dispersed polymeric species to Mo^{4+}. The position of this peak is in agreement with that observed in previous reports [35] where Ni and Mo were deposited at acidic pH (pH ~ 1.5) over an alumina support. Going from NMP(0) to NMP(7) a decrease of about ~20 °C (regarding the temperature at which the aforementioned phenomenon took place) suggested that more reducible species were present in the latter. This fact could be originated in diminished interaction between deposited molybdates and the alumina support, when EG was used as additive during simultaneous Ni–Mo–P impregnation. The second signal, identified in the 500–447 °C range, could be ascribed to oxidic Ni^{2+} species (being directly reduced with no intermediaries to Ni^0 [36]) in low interaction with the alumina carrier. By increasing EG concentration in the impregnating solution

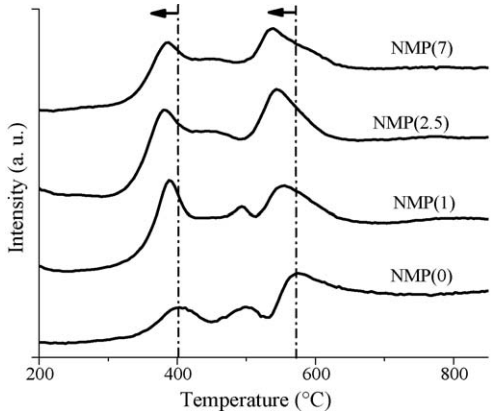

Fig. 8. Temperature-programmed reduction profiles of dried P-doped $NiMo/Al_2O_3$ samples prepared at various EG/Ni ratios. Thermogram corresponding to a similar material prepared with no ethyleneglycol included as reference.

Table 1
Temperature of maximum of main signals registered from TPR (temperature-programmed reduction) profiles for various P-doped $NiMo/Al_2O_3$ impregnated precursors (dried at 120 °C) prepared with or without ethyleneglycol.

Sample	T_{max} (°C)		
	$Mo^{6+} \rightarrow Mo^{4+}$	$Ni^{2+} \rightarrow Ni^0$	$Mo^{4+} \rightarrow Mo^0$
NMP(0)	403	500	576
NMP(1)	388	493	552
NMP(2.5)	384	451	543
NMP(7)	384	447	539

T_{max}, temperature of maximum in the corresponding signal.

used to prepare various formulations, both a shift to lower temperature (see Table 1) and a diminution in the intensity if the corresponding signals were observed. In NMP(7) Ni^{2+} reduction appeared just as a shoulder of the first peak observed (that corresponded to Mo^{6+} to Mo^{4+} reduction). It is possible that for the formulations where higher EG concentration was used during catalyst synthesis the signal originated in Ni^{2+} transformation to Ni^0 could be merged to that belonging to poly-molybdates reduction (the one registered at the lowest temperature) being then undistinguishable. Again, decreased interaction between impregnated species (in this case, nickel-containing ones) and the Al_2O_3 substrate was suggested. EG simultaneously impregnated with Ni, Mo and P seemed to be playing a leading role on the observed behavior. Finally, the peak which maximum was registered at the highest temperature (in the 539–576 °C range, depending on the formulation) could be related to further reduction of Mo^{4+} species to Mo° [35]. Tetrahedral molybdates reduction could also contribute to the aforementioned signal, mainly in the case of the sample prepared with no organic additive where those anions could be originated by decomposition of pentamolybdates originally present in the impregnating solution [34]. It is worth mentioning, however, that this signal was registered at a temperature considerably lower to that reported for that kind of phenomenon in the case of a $NiMo/Al_2O_3$ formulation submitted to calcining [35]. Thus, it seemed that by avoiding high-temperature annealing (preparation step eliminated to preserve organic additive integrity), the presence of molybdenum species in high interaction with the support was precluded, this being reflected in lower temperature of metallic Mo formation. Presumably, these more weakly bounded deposited phases could lead to increased sulfidability after treatment under H_2S/H_2 at 400 °C (see Section 2.1) that could in turn be reflected in higher proportion of species active in hydrodesulfurization reactions.

3.4. High-resolution transmission electron microscopy (HR-TEM)

In electron micrographs shown in Fig. 9(a)–(d), morphology of supported MoS_2 particles over various sulfided catalysts prepared (with and without EG) are shown. Average stacking degree slightly decreased in samples prepared in presence of higher ethyleneglycol concentration (NMP(2.5) and NiMoP(7)), respecting the formulation synthesized with no additive (see Table 2). Meanwhile, diminution in average slab length in catalysts modified by EG was more evident. Mazoyer et al. [9] reported no important effect of added di-ethyleneglycolbutylether (at mol ratio Mo/additive = 0.75, equivalent to additive/promoter = 3.3) on MoS_2 particles morphology, during the modification of a commercial P-doped $CoMo/Al_2O_3$ catalyst. Those authors registered slight increases (of about ~10%) in average stacking degree (from 1.8 to 2.0) and slab length (from 2.5 to 2.7 nm) due to the influence of the organic agent. On the other hand, Iwamoto et al. [11] attributed the enhanced HDS activity of $CoMo/Al_2O_3$ formulations modified by polyethylene glycol (PEG at 10 wt%) to increased dispersion of

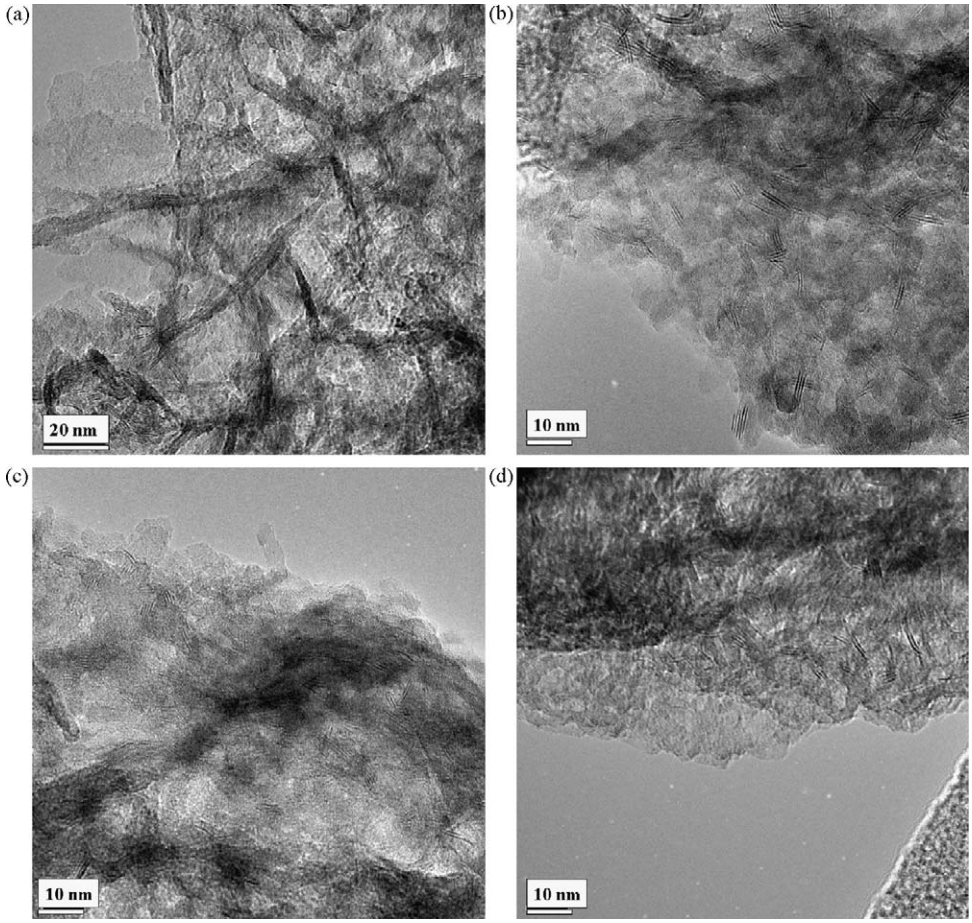

Fig. 9. High-resolution transmission electron micrographs of sulfided P-doped NiMo/Al_2O_3 catalysts prepared with or without organic additive, showing MoS_2 particles morphology. (a) NMP(0); (b) NMP(1); (c) NMP(2.5); (d) NMP(7).

molybdenum sulfide crystallites originated by effect of the organic additive. In this case, higher stacking was observed in the conventional formulation where no organic agent was added during catalyst synthesis. In the opposite to that reported in [9], mainly monolayered particles were identified in the catalysts where PEG was used during preparation even though the prototype was submitted to high-temperature calcining (at 550 °C under air) that provoked organic species combustion. Presumably, the effect of glycol addition on the supported MoS_2 particles morphology was still evident in spite of the aforementioned treatment carried out before transformation of the oxidic supported phases to the corresponding sulfided ones.

3.5. X-ray photoelectron spectroscopy (XPS) analysis

The XPS profiles of Mo 3d region for various sulfided NiMoP/alumina catalysts studied are shown in Fig. 10(a)–(d). Proper deconvolution of the registered peaks provided the data summarized in Table 3. Mo signals were fitted considering doublets (corresponding to $3d_{5/2}$ and $3d_{3/2}$ contributions) due to Mo^{6+} (from oxidic molybdenum), Mo^{5+} (oxysulfide species) and Mo^{4+} (from MoS_2) and taking into account the criteria proposed by Beccat et al. [37]. From the pertinent data, it was determined that both molybdenum dispersion (as a function of Mo_T/Al ratio where $Mo_T = Mo^{6+} + Mo^{5+} + Mo^{4+}$) and sulfidability (expressed as Mo^{4+}/Mo_T ratio) decreased by augmenting EG concentration in the impregnating solution, during preparation of various formulations. In this line, Mazoyer et al. [9] determined lower molybdenum sulfidability after treatment under H_2S/H_2 at temperature $\leq$200 °C) in samples of alumina-supported P-doped CoMo catalyst with tri-ethyleneglycol butyl ether as modifier, although after sulfiding at more severe conditions the S/(Co + Mo) ratio slightly increased, as to that of the formulation prepared without organic agent. Also, Nicosia and Prins [8] found that for materials sulfided at 350 °C $< T$ Mo–S coordination number was lower in Co–Mo–P catalyst (with alumina carrier) simultaneously impregnated with tri-ethylene glycol, as compared to the corresponding sample synthesized with no organic agent. After activation at more severe conditions, however, enhanced Mo–S coordination number was registered in the material impregnated with organic additive. In this case, delayed molybdenum sulfidation was attributed to strong interaction of this species with the organic additive that needed to be thermally decomposed to allow increased transformation of Mo^{6+} to Mo^{4+}. In our case, we could not discard that in our catalysts some unknown highly stable glycol-derived species (see Section 3.1 and

Table 2
Average slab length and stacking degree (as determined by high-resolution transmission electron microscopy) of MoS_2 phase crystallites present on sulfided P-doped sulfided NiMo/Al_2O_3 catalysts prepared with or without ethyleneglycol.

Sample	Slab length (nm)	Stacking number
NiMoP(0)	6.5	3.4
NiMoP(1)	4.8	3.7
NiMoP(2.5)	3.9	3.2
NiMoP(7)	4.8	3.1

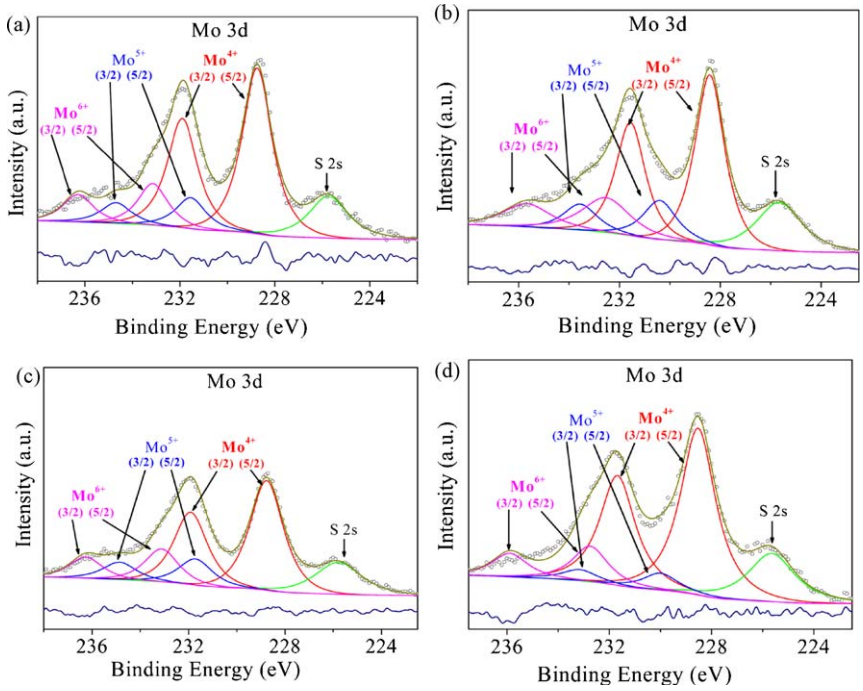

Fig. 10. XPS envelope of Mo 3d region of sulfided P-doped NiMo/Al_2O_3 catalysts prepared with or without organic additive. Peak deconvolution to various Mo species also shown. (a) NMP(0); (b) NMP(1); (c) NMP(2.5); (d) NMP(7).

Table 3
Surface molybdenum, phosphorous and carbon species over various P-doped NiMo/alumina sulfided catalysts prepared with or without ethyleneglycol, as determined by XPS analysis. C/Al represents the areal ratio of C signal at BE = 288.1–288.9 eV, over Al peak.

Sample	Mo^{4+}/Al	Mo^{5+}/Al	Mo^{6+}/Al	Mo_T/Al	Mo^{4+}/Mo_T	P/Al	C/Al
NMP(0)	0.049	0.009	0.012	0.070	0.70	0.024	–
NMP(1)	0.041	0.011	0.014	0.066	0.62	0.013	0.053
NMP(2.5)	0.033	0.008	0.010	0.051	0.65	0.017	0.043
NMP(7)	0.022	0.009	0.007	0.038	0.58	0.018	0.077

Mo_T (total surface molybdenum) = Mo^{4+} + Mo^{5+} + Mo^{6+}.

thermograms in Fig. 3) could stand H_2S/H_2 treatment at temperature up to 400 °C, hindering at some extent MoS_2 formation. Regarding Mo dispersion, Nicosia and Prins [8] reported increased Mo–Mo coordination (as determined by in situ QEXAFS) by using tri-ethylene glycol as additive in alumina-supported sulfided CoMo catalysts. This effect could be related to Mo species of larger crystallite size, this being in full agreement with decreased dispersion found in our materials prepared in presence of ethyleneglycol (see Table 3). These results seemed to be contradictory when those from our HR-TEM studies (see Section 3.4 and Table 2) are taking into account. However, it should be considered that although HR-TEM is considered a valuable tool to estimate supported phases dispersion in HDS catalyst, even in the best cases just about 10% of the total active phase is detectable [38] mainly due to interferences arising from the carrier. Invisibility is principally due to inadequate slabs orientation respecting to the electron beam, thickness effects of the catalyst section analyzed and inability of most of the microscopes to detect the smallest MoS_2 structures [39]. Even more, MoS_2 slabs edge-bonded to the carrier surface could be easily identified whereas basal-bonded layers could remain undetectable [40]. Interestingly, enhanced reducibility of Mo^{6+} species to Mo^{4+} (under H_2/Ar stream, see Section 3.3 temperature-programmed reduction, Fig. 8 and Table 1) in materials impregnated in presence of the organic modifier was not reflected in increased sulfidability (under H_2S/H_2 at 400 °C). Interestingly, enhanced reducibility of Mo^{6+} species to Mo^{4+} (under H_2/Ar stream, see Section 3.3. Temperature-programmed reduction, Fig. 8 and Table 1) in materials impregnated in presence of the organic modifier was not reflected in increased sulfidability (under H_2S/H_2 at 400 °C). In this regard, Massoth [41] has reported that by varying the alumina carrier phase (γ or η) Mo-support interaction could differ depending on the substratum acidity. That parameter affected more clearly Mo sulfidability than its reduction under H_2, pointing out to differences in the sensitivity of these reactions to Mo-carrier inter-bonding strength, as our results also suggested.

Phosphorous dispersion (expressed as function of P/Al signal ratio) was also quantified (see column 7 of Table 3). Clearly, this parameter decreased with the EG concentration in the impregnating solution. This could be considered an indication of polyphosphates formation in samples prepared with organic additive. In the past, Nicosia and Prins [42] have proposed that during impregnation on γ-alumina tri-ethylene glycol favored the formation of polyphosphates and $PMo_{12}O_{40}^{3-}$ heteropolymolybdate species, from $P_2Mo_5O_{23}^{6-}$ anions originally present in the impregnating solution. They considered, following the way of reasoning of van Eck et al. [43], that phosphate polymerization was favored when the support surface was not able to accommodate PO_4 species in monolayer. In accordance with this, decreased surface area of the alumina carrier impregnated in presence of

Table 4
Nickel surface species of various P-doped NiMo/alumina sulfided catalysts prepared with or without ethyleneglycol, as determined by XPS analysis.

Sample	NiS_x/Al	NiMoS/Al	Ni_{Ox}/Al	Ni_T/Al	Ni_S/Ni_T	PR	$(Ni/Mo)_{slabs}$
NMP(0)	0.0011	0.0037	0.0028	0.0076	0.63	48.8	0.076
NMP(1)	0.0016	0.0056	0.0029	0.0101	0.71	55.3	0.137
NMP(2.5)	0.0009	0.0032	0.0025	0.0066	0.62	48.7	0.097
NMP(7)	0.0028	0.0043	0.0021	0.0092	0.77	46.2	0.195

Ni_{Ox}, oxidic nickel, Ni_S, sulfidic nickel = NiS_x + NiMoS. Ni_T (total surface Ni) = NiS_x + NiMoS + Ni_{Ox}. $Ni_S/Ni_T = 1 - (Ni_{Ox}/Ni_T)$. PR (promotion rate) = $(NiMoS/Ni_T) \times 100$. $(Ni/Mo)_{slabs}$ = promoter ratio = $NiMoS/Mo^{4+}$.

ethyleneglycol could then favor polyphosphate formation. This could be in agreement with our FTIR spectra of NMP(0) and NMP(1) impregnated samples (see Fig. 7 and Section 3.2) where the latter showed decreased absorption band corresponding to Al–O–P linkages related to non-stoichiometric aluminum phosphate.

Regarding deposited carbonaceous remains, Mazoyer et al. [9] determined that after sulfiding (under H_2S/H_2 flow) at 300 °C, essentially all carbon was removed in an alumina-supported commercial CoMoP formulation modified by di-ethyleneglycolbutylether addition. In our case, although we did not quantified C by XPS (due to the effect of adventitious carbon) it is worth mentioning that in sulfided catalysts prepared in presence of glycol one additional signal due to carbonaceous species could be identified. In various samples this peak was registered at binding energy of 288.1–288.9 eV (as referred to C 1s signal at 284.6 eV related to adventitious carbon). Even more, the intensity of that signal (expressed as C/Al areal ratio, see column 8 of Table 3) increased with the concentration of EG in the impregnation solutions used during catalyst preparation. According to some authors [44], tail and shoulders that could appear additionally to the peak attributed to graphitic carbon during XPS analysis could be related to oxygen-containing functional groups on the carbon surface. In addition, other investigators [45] have reported a peak at 288.9 eV (that nicely agreed with that we found in the XPS spectra of our sulfided catalysts modified by EG addition) in chemically oxidized activated carbon cloths, this signal being ascribed to O–C=O (carboxyl or ester groups). In this line, Frizi et al. [46] assigned a XPS peak at ~289 eV to the C 1s core level of carboxyl groups, from thermal decomposition of the thioglycolic acid used as additive to improve the properties of a commercial alumina-supported CoMo catalyst. In our case, as those carboxyl groups did not originally exist in the added ethyleneglycol it seemed that they could have been somehow formed under the conditions utilized during various catalyst preparation steps. In this regard, for alumina-supported nickel samples prepared with Ni(II)-ethylenediamine complexes ($[Ni(en)_2(H_2O)_2](NO_3)_2$ and $[Ni(en)_3](NO_3)_2$) and submitted to thermal treatment under inert atmosphere it was determined that the C 1s XPS pattern of carbon residua had a shoulder at 289.5 eV related to C=O functional groups [47]. As species containing carbonyl were initially absent in this case, it was assumed that partial ethylenediamine ligands oxidation could occur during nitrates decomposition.

Also, by characterizing ZrO_2–TiO_2 mixed oxides prepared through the so-called glycol thermal method it was found [48] that materials prepared in presence of ethyleneglycol contained refractory carbonaceous deposits that were eliminated by combustion at 500 °C (under air atmosphere), this fact being more evident in samples of higher titania content. In the opposite, for similar solids synthesized with 1,4-butanediol recalcitrant organic remains were absent, suggesting that deposition of carbon could be dictated by distinctive interactions between the specific organic compound used and the carrier surface. In our case, we could hypothesize that the high-temperature exothermicity observed (maximum at ~438 and ~448 °C, for NiMoP(1) and NiMoP(7), respectively) in thermal profiles shown in Fig. 3 could probably be originated in the combustion of some oxygen-containing refractory carbonaceous species. Perhaps those carbonaceous deposits could be playing a role on hindering Mo^{6+} sulfidation, as determined from the corresponding XPS analysis (see column 5 of Table 3). Deeper studies in this direction are obviously needed.

Respecting analysis of surface Ni species (see Fig. 11), the Ni 2p envelope was decomposed by considering three major contributions [49] corresponding to NiS_x sulfided phase (which could arise from Ni_2S_3, Ni_9S_8 or NiS, with binding energy between 853.5 and 853.8 eV), to oxidic nickel on the Al_2O_3 carrier (binding energy of ~856.9 eV) and the so-called NiMoS phase (with binding energy between 854.6 and 855.0 eV). Regarding oxidic nickel in our non-calcined samples, the binding energy of the corresponding signal (~856.9 eV) did not match that of NiO (~833.5 eV) being closer to that characteristic of $Ni(OH)_2$ [50]. Interestingly, the trends observed for surface Ni species (see Table 4) were the opposite to those found for deposited molybdenum. In general, both nickel dispersion (as represented by N_T (total surface nickel)/Al) and sulfidability (expressed as Ni_S/Ni_T ratio equivalent to the proportion of sulfided nickel over total surface Ni) clearly increased with EG amount concentration on the Ni–Mo–P impregnating solution. Both parameters were augmented in about ~21% by going from NMP(0) to NMP(7). Other authors [9] have found (by characterizing through XANES and EXAFS) that di-ethyleneglycolbutylether addition delayed Co sulfidation at low temperature (~100 °C) in alumina-supported CoMoP, the sulfur coordination of cobalt being about half to that of a reference catalysts non-modified by organic compound addition. Nevertheless, at $T \sim 150$ °C both catalysts had approximately the same S coordination (that was considered a measure of sulfiding degree). After sulfidation at more severe conditions, however, those investigators did not identified a significant effect of the organic agent added on the transformation of oxidic cobalt to the sulfidic phase. It is worth mentioning that in this case, total conversion of deposited cobalt to the corresponding sulfided phases was achieved for both studied materials. Opposing to that aforementioned, Nicosia and Prins [8] found important differences regarding the low-temperature sulfiding behavior of CoMoP/alumina materials by tri-ethyleneglycol (TEG) addition during catalyst preparation. At $T < 120$ °C, sulfiding degree was increased in the catalysts modified by the organic additive. The shift to lower temperature registered for Co sulfidation was attributed to decreased cobalt–alumina carrier interaction originated in TEG deposition. Indeed, this fact could preclude formation of refractory hardly sulfidable Co species. In spite of this, at more severe conditions (~230 °C) the effect of TEG was less evident because in any case 100% Co transformation to the sulfided phase was gotten. Expectedly, the effect of EG addition on promoter sulfidation could be dependent on the preparations step where the organic modifier is added (simultaneous Co–Mo–P–glycol deposition in [8] *versus* modification of a commercial formulation by impregnation with glycol in aqueous solution in [9]). A similar reason to that provided by Nicosia and Prins [8] could be invoked in our case to explain increased nickel sulfidation in our catalyst prepared with ethyleneglycol, where addition of the organic additive could result in Ni species of weakened interaction with the

alumina support (see Fig. 8 and Section 3.3). It is worth noting that, differently to that reported in the aforementioned works [8,9], nickel in our catalysts was not totally sulfided after treatment at 400 °C by 2 h under H_2S/H_2 stream (see column 6 of Table 4), making more evident the beneficial effect of EG addition.

Two parameters considered of the highest relevance in determining the hydrodesulfurizating properties of sulfided NiMo catalysts are the promotion rate (PR) and the promoter ratio (see the corresponding formulas in the footnote of Table 4). The former represents the proportion of total deposited nickel that is actually engaged in the NiMoS phase formation meanwhile the latter is related to the amount of that highly active species [49]. Regarding PR values determined for various catalysts studied (see column 7 of Table 4), no beneficial effect of ethyleneglycol addition was clearly evident. This meant that although the proportion of sulfided nickel progressively augmented by adding incremental amounts of the organic modifier (during Ni–Mo–P impregnation), most of that sulfidic Ni corresponded to Ni_2S_3, Ni_9S_8 or NiS species segregated from the MoS_2 phase. If we take into account the decreased dispersion and sulfidability of surface molybdenum resulting from using EG additive (columns 5 and 6 of Table 3, respectively), the aforementioned fact could be originated by (among other factors) the limited amount of molybdenum sulfide edges available to be "decorated" by sulfidic nickel integration (thus being able to originate the "NiMoS phase"). Although in alumina-supported Ni–Mo–P sulfided materials the proportion of total surface nickel that participated in NiMoS phase ("promotion rate") slightly decreased by augmenting EG concentration in the impregnating solution (see column 7 of Table 4), the absolute amount of that highly active phase ("promoter ratio", column 8, Table 4) was clearly enhanced by modifying the original catalyst formulation by using impregnating solutions (Ni–Mo–P) of incremental ethylene glycol concentration. This fact could contribute to explain enhanced desulfurizating properties that had been reported in the past for catalysts modified by glycolic compounds addition [5–7]. In full agreement with that we found, other authors [9] have invoked improved integration of the cobalt promoter in CoMoP/alumina catalysts (by glycol addition) as the main reason of enhanced activity in the 4,6-dimethyl-dibenzothiophene HDS. Even more, those investigators [9] considered augmented selectivity to the product from direct desulfurization [51] as evidence of more efficient promoter integration to the MoS_2 phase. Following the way of reasoning of Nicosia and Prins [42], during impregnation on alumina and in absence of glycols $P_2Mo_5O_{23}^{6-}$ could be decomposed to phosphates and MoO_4^{2-} [52]. As these molybdates preferably react with surface basic hydroxyls, their adsorption probability is strongly decreased when in presence of tri-ethyleneglycol (which also could react with basic OH's). Thus, the Mo/P ratio in the impregnating solution could be raised, this fact resulting in $PMo_{12}O_{40}^{3-}$ anions formation. By ^{31}P NMR spectroscopy it has been shown [7] that in silica- and alumina-supported CoMoP catalysts prepared in presence of tri-ethyleneglycol (TEG) Co and Mo are in close interaction where the former acts as counter-cation, the final result being improved decoration of MoS_2 slabs in the final sulfided catalyst. In the same line, Griboval et al. [53] showed that those Keggin-type phosphomolybdate anions could form cobalt complexes ($Co_{3.5}PMo_{12}O_{40}$, for instance) leading to enhanced MoS_2 slabs decoration by promoter atoms. In addition, Nicosia and Prins [42] proposed that during impregnation in presence of TEG glycol species where phosphomolybdate anions could be complexing Co^{2+} cations could be preserved on the alumina surface, enhancing then formation (after sulfiding) of more homogeneous Co–Mo–S type II structures. From our XPS data, we could hypothesize that similar facts to those aforementioned could explain the enhanced formation of NiMoS phases in our catalysts modified by EG impregnation. Further investigations including additional materials characterization are in due course to try to shed light in this direction.

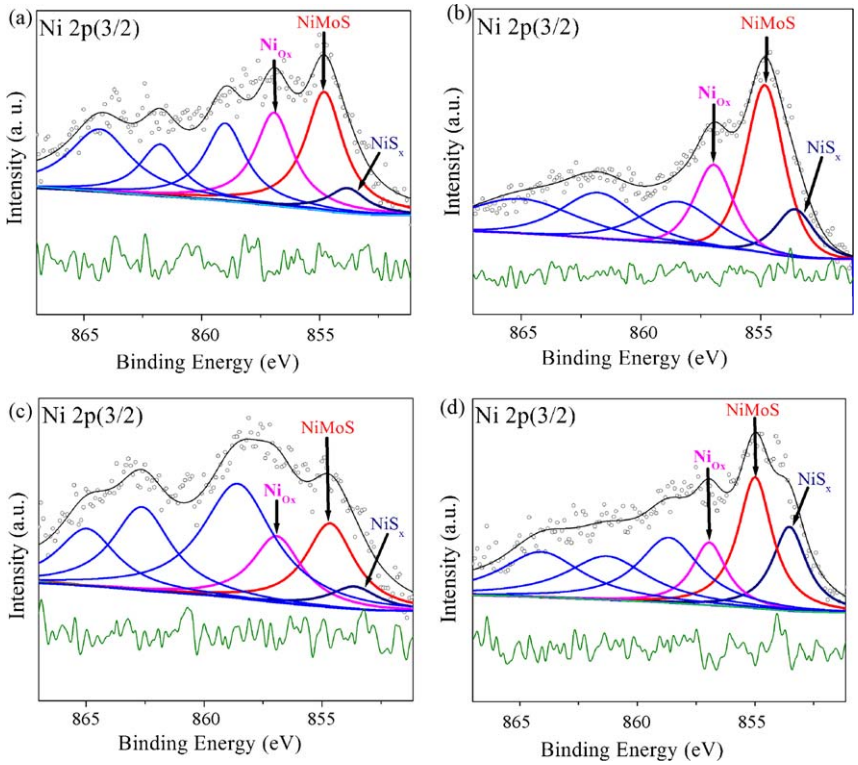

Fig. 11. XPS envelope of Ni $2p_{3/2}$ region of sulfided P-doped NiMo/Al_2O_3 catalysts prepared with with or without organic additive. Peak deconvolution to various Ni species also shown. (a) NMP(0); (b) NMP(1); (c) NMP(2.5); (d) NMP(7).

3.6. HDS reaction tests

Expectedly, increased amounts of "NiMoS phase" in our catalyst prepared with ethyleneglycol modifier could be reflected in augmented HDS properties. Thus, a detailed study on their HDS capabilities was undertaken, including catalytic testing in presence of both model system (dibenzothiophene in *n*-hexadecane) and real feedstock (straight-run gas oil from Mexican crude oil). Although a detailed report on the results of these investigations will be the matter of an oncoming report, some important findings are pertinent at this point in order to evidence the potential of using ethyleneglycol in obtaining HDS catalysts of improved desulfuration capability. To this end, liquid-phase dibenzotiophene (DBT) HDS was carried out in a batch reactor (T = 320 °C, P = 70 kg/cm^2) by using a previously described protocol [54]. Product analyses were carried out by gas chromatography as described in [55]. Catalytic activity of sulfided NiMoP(0) and NiMoP(1) samples (activated in gas-phase, as described in Section 2.1) was compared in a pseudo-first-order kinetic constant basis [54], where the determined values were $k_{HDSDBT} = 1.18 \times 10^{-4}$ and 1.33×10^{-4} (in m^3/(kg$_{cat}$ s), respectively. The magnitude of this activity improvement was very similar to that reported by Nicosia and Prins when comparing the performance of sulfided Co–Mo–P/Al_2O_3 catalysts (in gas-phase thiophene HDS at 350 °C) simultaneously impregnated with ethyleneglycol (at EG/Co = 1.76), with that of a corresponding non-modified conventional formulation. In our case, no significant differences in selectivity over the two catalysts were observed, where biphenyl (from the direct desulfurization route [56]) was the major product (~83% selectivity at 30% conversion) the rest of DBT being converted to cyclohexylbenzene (Fig. 11).

We also tested the aforementioned formulations in straight-run gas oil (SRGO, from a Mexican crude) desulfurization. The properties of this feedstock are shown in Table 5. HDS tests were carried out in a fixed-bed up-flow reactor (316 stainless steel, 3/8 in. diameter, coaxial 1/8 in. thermo-well, 100 ml of loaded catalyst). Dried (Ni + Mo + P)/Al_2O_3 impregnated with and without ethyleneglycol (at EG/Ni = 1) were in situ liquid-phase sulfided at 340 °C (3 h). SRGO (1.68% S, see Table 5) was spiked with dimethyldisulfide to a total S content of ~2.68 wt%. This stream was fed to the reactor according to an LHSV = 1.5 h^{-1}. Pressure was set to 27.2 kg/cm^2 meanwhile a H_2/oil ratio = 1873 ft^3/bbl was kept. After catalyst activation, the reactor feed was switched to non-spiked SRGO (1.68% S). Operating conditions were: T = 350 °C, P = 70 kg/cm^2, LHSV = 1.5 h^{-1} and H_2/oil = 2500 ft^3/bbl. It is worth mentioning that these parameters closely correspond to those used in industrial hydrotreaters used in ultra-low sulfur diesel (ULSD) production. H_2S by-product dissolved in hydrotreated gas oil samples was stripped-off by N_2 bubbling. S concentration in liquid samples was determined by UV fluorescence (ASTM-D 5453-04) [55]. Results from these real-feedstock HDS experiments are summarized in Fig. 12. At LHSV = 1.5 h^{-1} the average S content in gas oil hydrotreated over NMP(0) was of about 358 ppm, this value descending to ~104 ppm at higher severity (decreased space velocity). For NMP(1) the corresponding sulfur concentrations at the aforementioned operating conditions were of ~245 and ~7 ppm, respectively. Thus, it was proven that at the highest contact time (LHSV = 1 h^{-1}) the sulfided catalyst modified by simultaneous ethylene glycol addition during Ni–Mo–P impregnation enabled obtaining ULSD from a Mexican SRGO (16 800 ppm initial S content). Even more, the advantage of the material prepared in presence of the organic compound was highly pronounced in the removal of sterically hindered compounds (i. e., DBT's alkylated in 4 and/or 6 positions) that constitute the most recalcitrant organo-S compounds present in oil-derived middle distillates. This fact could be originated by various factors, for instance, better response of modified catalyst in aromatic rings hydrogenation reactions (requirement to enhance transformation of the aforementioned alkylated DBT's), or improved removal of HDS reactions inhibitors (as organo-N compounds [55] or poly-aromatics [57]), among others. A more detailed study on this matter and on the effect of increased amount of additive on HDS performance is required and will be addressed in an oncoming report.

Table 5
Properties of the straight-run gas oil (from a Mexican crude) used during the real feedstock HDS catalytic test.

Property		Method
IBP[a] (°C)	184.5	ASTM D-86
20%V (°C)	242.0	
40%V (°C)	264.8	
60%V (°C)	283.8	
80%V (°C)	310.8	
FBP[b] (°C)	354.4	
Specific weight 20/4 (°C/°C)	0.8434	ASTM D-4052
S (wt%)	1.68	ASTM D-4294
Total N (ppm)	252	ASTM D-4629
Total aromatics (wt%)	30.6	ASTM D-5186
Monoaromatics (wt%)	20.8	
Diaromatics (wt%)	8.2	
Polyaromatics (wt%)	1.6	
Bromine number (g_{Br}/100 g)	3.43	ASTM D-1159
Cetane index	50.8	ASTM D-976

[a] Initial boiling point.
[b] Final boiling point.

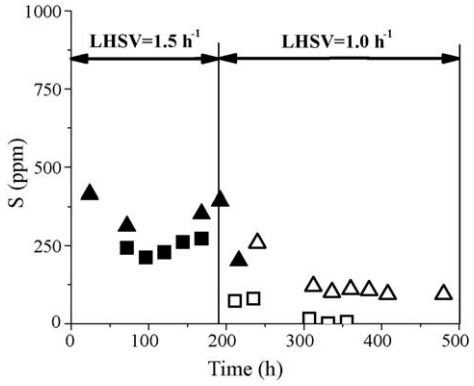

Fig. 12. S concentration in products (ppm) from hydrotreatment of straight-run gas oil (from a Mexican Crude) over NMP(0) and NMP(1) catalysts, *versus* time on stream. Flow reactor, P = 70 kg/cm^2, T = 350 °C, LHSV = 1.0 and 1.5 h^{-1}, H_2/oil = 2500 ft^3/bbl. Triangles: NMP(0); squares: NMP(1). Filled symbols: at LHSV = 1.5 h^{-1}; blank symbols: at LHSV = 1.0 h^{-1}.

4. Conclusions

The ethyleneglycol/Ni ratio (1, 2.5 or 7) in the aqueous impregnating solution used to simultaneously impregnate Ni, Mo and P over a commercial alumina support exerted a determining influence on the surface and structural properties of the corresponding sulfided P-doped NiMo/Al_2O_3 hydrodesulfurization catalysts. As determined by temperature-programmed reduction, ethyleneglycol addition during impregnation resulted in decreased interaction between deposited phases (Mo and Ni) and the alumina carrier. Dispersion and sulfidability (as observed by XPS) of molybdenum and nickel showed opposite trends when incremental amounts of the organic compound were added during catalysts preparation. Meanwhile Mo sulfidation was progressively decreased by augmenting EG concentration in the impregnating solution, more dispersed sulfidic nickel was evidenced in materials synthesized at higher EG/Ni ratios. Also, formation of the

so-called "NiMoS phase" was enhanced by increasing the amount of added ethyleneglycol during simultaneous Ni–Mo–P–EG deposition over an alumina carrier. This fact was reflected in enhanced activity in both liquid-phase benzothiophene HDS (batch reactor) and straight-run gas oil desulfurization (steady-state flow reactor), the latter test carried out at conditions similar to those used in industrial hydrotreaters for the production of ultra-low sulfur diesel.

Acknowledgements

The authors appreciate financial support from Instituto Mexicano del Petróleo (R&D Project D.00446). M.C. Barrera also acknowledges Instituto Mexicano del Petróleo (88404), CONACYT (88474, Mexico) and ICyT for a Post Doctoral fellow grant.

References

[1] E. Ito, J.A.R. van Veen, Catal. Today 116 (2006) 446–460.
[2] A.J. van Dillen, R.J.A.M. Terörde, D.J. Lensveld, J.W. Geus, K.P. de Jong, J. Catal. 216 (2003) 257–264.
[3] G. Kishan, L. Coulier, V.H.J. de Beer, J.A.R. van Veen, J.W. Niemantsverdriet, J. Chem. Soc. Chem. Commun. 13 (2000) 1004–1103.
[4] M. Sun, D. Nicosia, R. Prins, Catal. Today 86 (2003) 173–189.
[5] Y. Uragami, E. Yamaguchi, H. Yokozuka, K. Uekusa, US Patent 6,280,610 (2001).
[6] F.L. Plantenga, S. Eijsbouts, M.B. Cerfontain, PCT WO 02/04117 A1 (2002).
[7] D. Nicosia, R. Prins, J. Catal. 229 (2005) 424–438.
[8] D. Nicosia, R. Prins, J. Catal. 231 (2005) 259–268.
[9] P. Mazoyer, C. Geantet, F. Diehl, C. Pichon, T.S. Nguyen, M. Lacroix, Oil&Gas Sci. Tech. Rev. IFP 60 (2005) 791–799.
[10] V. Costa, K. Marchand, M. Digne, C. Geantet, Catal. Today 130 (2008) 69–74.
[11] R. Iwamoto, N. Kagami, A. Iino, J. Jpn. Petrol. Inst. 48 (2005) 237–242.
[12] A.L. Dicks, R.L. Ensell, T.R. Phillips, A.K. Szczepura, M. Thorley, A. Williams, R.D. Wragg, J. Catal. 72 (1981) 266–273.
[13] T. Fujikawa, O. Chiyoda, M. Tsukagoshi, K. Idei, S. Takehara, Catal. Today 45 (1998) 307–312.
[14] Thermo VG-Scientific. XPS and Auger Handbook. Doc. Number: 600001, issue 2 (2003).
[15] L. Saravanan, S. Subramanian, J. Colloid Interface Sci. 284 (2005) 363–377.
[16] S. Braun, L.G. Appel, M. Schmal, Catal. Commun. 6 (2005) 7–12.
[17] I.C. Leite, S. Braun, M. Schmal, J. Catal. 223 (2004) 114–121.
[18] L. Espinosa-Alonso, K.P. de Jong, B.M. Weckhuysen, J. Phys. Chem. C 112 (2008) 7201–7209.
[19] Y. Chen, W. Zhou, Z. Shao, N. Xu, Catal. Commun. 9 (2008) 1418–1425.
[20] X. Ma, J. Gong, X. Yang, S. Wang, Appl. Catal. A 280 (2005) 215–223.
[21] W.M. Shaheen, Mater. Lett. 52 (2002) 272–282.
[22] H. Matuura, T. Miyazawa, Bull. Chem. Soc. Jpn. 40 (1967) 85–94.
[23] S.B. Hong, M.A. Camblor, M.E. Davis, J. Am. Chem. Soc. 119 (1997) 761–770.
[24] J.A.R. van Veen, Ms.P.C. de Jong-Versloot, G.M.M. van Kessel, F.J. Fels, Thermochim. Acta 152 (1989) 359–370.
[25] J.A.R. van Veen, G. Jonkers, W.H. Hesselink, J. Chem. Soc., Faraday Trans. 1 (85) (1989) 389–413.
[26] G. Ramis, G. Busca, V. Lorenzelli, J. Chem. Soc. Faraday Trans. 1 (83) (1987) 1591–1599.
[27] W. Zhang, M. Sun, R. Prins, J. Phys. Chem. B 106 (2002) 11805–11809.
[28] A.A. Tsyganenko, P.P. Mardilovich, J. Chem. Soc. Faraday Trans. 92 (1996) 4843–4852.
[29] P.C.H. Mitchell, S.A. Wass, Appl. Catal. A 225 (2002) 153–165.
[30] Y. Liu, Z. Shi, L. Zhang, Y. Fu, J. Chen, B. Li, J. Hua, W. Pang, Chem. Mater. 13 (2001) 2017–2022.
[31] V. Siva Kumar, A.H. Padmasri, C.V.V. Satyanarayana, I. Ajit Kumar Reddy, B. David Raju, K.S. Rama Rao, Catal. Commun. 7 (2006) 745–751.
[32] F. Yaripour, F. Baghaei, I. Schmidt, J. Perregaard, Catal. Commun. 6 (2005) 542–549.
[33] L. Pettersson, I. Andersson, L.O. Öhman, Inorg. Chem. 25 (1986) 4726–4733.
[34] H. Kraus, R. Prins, J. Catal. 164 (1996) 251–259.
[35] R. López Cordero, A. López Agudo, Appl. Catal. A 202 (2000) 23–35.
[36] R. Molina, G. Poncelet, J. Catal. 173 (1998) 257–267.
[37] P. Beccat, P. Da Silva, Y. Huiban, S. Kasztelan, Oil&Gas Sci. &Tech. Rev. IFP 54 (1999) 487–496.
[38] M. Perez De la Rosa, S. Texier, G. Berhault, A. Camacho, M.A. Yacamán, A. Mehta, S. Fuentes, J.A. Montoya, F. Murrieta, R.R. Chianelli, J. Catal. 224 (2004) 288–299.
[39] S. Eijsbouts, Appl. Catal. A 158 (1997) 53–92.
[40] R.R. Chianelli, Oil&Gas Sci. Tech. Rev. IFP 61 (2006) 503–513.
[41] F.E. Massoth, J. Catal. 36 (1975) 164–184.
[42] D. Nicosia, R. Prins, J. Catal. 234 (2005) 414–420.
[43] E.R.H. van Eck, A.P.M. Kentgens, H. Kraus, R. Prins, J. Phys. Chem. 99 (1995) 16080–16086.
[44] J.A. Maciá-Agulló, D. Cazorla-Amorós, A. Linares-Solano, U. Wild, D.S. Su, R. Schlögl, Catal. Today 102 (2005) 248–253.
[45] M. Polovina, B. Babić, B. Kaluderović, A. Dekanski, Carbon 35 (1997) 1047–1052.
[46] N. Frizi, P. Blanchard, E. Payen, P. Baranek, C. Lancelot, M. Rebeilleau, C. Dupuy, J.P. Dath, Catal. Today 130 (2008) 32–40.
[47] F. Négrier, E. Marceau, M. Che, J.-M. Giraudon, L. Gengembre, A. Löfberg, Catal. Lett. 124 (2008) 18–23.
[48] K. Kubo, S. Hosokawa, S. Furukawa, Sh. Iwamoto, M. Inoue, J. Mater. Sci. 43 (2008) 2198–2205.
[49] B. Guichard, M. Roy-Auberger, E. Devers, C. Legens, P. Raybaud, Catal. Today 130 (2008) 97–108.
[50] B.W. Hoffer, A.D. van Langeveld, J.-P. Janssens, R.L.C. Bonné, C.M. Lok, J.A. Moulijn, J. Catal. 192 (2000) 432–440.
[51] M. Breysse, G. Djega-Mariadassou, S. Pessayre, C. Geantet, M. Vrinat, G. Pérot, M. Lemaire, Catal. Today 84 (2003) 129–138.
[52] W.C. Cheng, N.P. Luthra, J. Catal. 109 (1988) 163–169.
[53] A. Griboval, P. Blanchard, E. Payen, M. Fournier, J.L. Dubois, Catal. Today 109 (1988) 163–169.
[54] J. Escobar, M.C. Barrera, J.A. de los Reyes, J.A. Toledo, V. Santes, J.A. Colín, J. Mol. Catal. A 287 (2008) 33–40.
[55] A. Alvarez, J. Escobar, J.A. Toledo, V. Pérez, M.A. Cortés, M. Pérez, E. Rivera, Fuel 86 (2007) 1240–1246.
[56] M. Houalla, N.K. Nag, A.V. Sapre, D.H. Broderick, B.C. Gates, AIChEJ 24 (1978) 1015–1021.
[57] E. Lecrenay, K. Sakanishi, I. Mochida, Catal. Today 39 (1997) 13–20.